THE JOURNAL OF BIOLOGICAL CHEMISTRY VOL. 282, NO. 33, pp. 24284–24293, August 17, 2007

Identification and Characterization of Vnx1p, a Novel Type of Vacuolar Monovalent Cation/H^+ Antiporter of *Saccharomyces cerevisiae*[*]

Received for publication, April 12, 2007, and in revised form, June 19, 2007 Published, JBC Papers in Press, June 22, 2007, DOI 10.1074/jbc.M703116200

Olivier Cagnac[‡], Marina Leterrier[‡], Mark Yeager[§], and Eduardo Blumwald[‡1]

From the [‡]Department of Plant Sciences, University of California, Davis, California 95616 and [§]Department of Cell Biology, The Scripps Research Institute, La Jolla, California 92037

We identified and characterized Vnx1p, a novel vacuolar monovalent cation/H^+ antiporter encoded by the open reading frame *YNL321w* from *Saccharomyces cerevisiae*. Despite the homology of Vnx1p with other members of the CAX (calcium exchanger) family of transporters, Vnx1p is unable to mediate Ca^{2+} transport but is a low affinity Na^+/H^+ and K^+/H^+ antiporter with a K_m of 22.4 and 82.2 mM for Na^+ and K^+, respectively. Sequence analyses of Vnx1p revealed the absence of key amino acids shown to be essential for Ca^{2+}/H^+ exchange. *vnx1*Δ cells displayed growth inhibition when grown in the presence of hygromycin B or NaCl. Vnx1p activity was found in the vacuoles and shown to be dependent on the electrochemical potential gradient of H^+ generated by the action of the V-type H^+-ATPase. The presence of Vnx1p at the vacuolar membrane was further confirmed with cells expressing a *VNX1::GFP* chimeric gene. Similar to Nhx1p, the prevacuolar compartment-bound Na^+/H^+ antiporter, the vacuole-bound Vnx1p appears to play roles in the regulation of ion homeostasis and cellular pH.

In *Saccharomyces cerevisiae* as well as in other eukaryotes and prokaryotes, K^+ is the most abundant cation and plays key roles in cellular ionic homeostasis and osmotic regulation. Potassium uptake is mediated mainly by the plasma membrane bond Trk1p and Trk2p. Trk1p, the high affinity K^+ transporter, seems to be predominant over Trk2p, since *trk1* mutants lose the ability to grow in low K^+ media (1, 2). Trk2p, the low affinity K^+ transporter, is able to substitute Trk1p activity only under K^+ limiting conditions or at low pH (3). Na^+ and other alkali cations enter the cell through K^+ uptake systems, and steady-state cytosolic Na^+ concentrations are established by the balance between Na^+ inward and Na^+ outward fluxes among the cytosol and the external medium or the vacuole.

In *S. cerevisiae* four *Ena* genes in tandem encode Na^+-ATPases that are the primary pathway for Na^+ exclusion (4). Several fungal Ena-type ATPases have been also described as K^+ efflux enzymes. *S. cerevisiae ena1-ena4* null mutants display lower Na^+ tolerance at alkaline pH than at acidic pH due to the presence of Nha1p, a plasma membrane-bound Na^+/H^+ antiporter (4, 5). Nha1p plays a role in pH regulation and also cell cycle regulation (6) and catalyzes the transport of Na^+ and K^+ with similar affinity ($K_m \approx 12$ mM). Similar to the $1Na^+/2H^+$ bacterial antiporters (7), Nha1p activity is electrogenic and induces a net charge movement across the membrane, whereas other eukaryotic Na^+/H^+ antiporters are electroneutral (8, 9).

Two other Nha1p homologues, Kha1p and Nhx1p, have been identified in *S. cerevisiae*. Kha1p has been described as a putative K^+/H^+ antiporter, and its deletion induced a growth defect at high external pH and hygromycin (10). Kha1p co-localized with Mntp1p, a Golgi-specific marker (11). Although Kha1p displays high amino acid sequence similarity to other Na^+/H^+ antiporters, its ability to mediate K^+/H^+ exchange has not been yet demonstrated. Nhx1p localizes to the pre-vacuolar compartment and function in the sequestration of sodium ions (K_m = 16 mM) by using the electrochemical proton gradient generated by the V-type H^+-ATPase in an electroneutral manner (12–14). Nhx1p can be also localized to discrete patches at the vacuolar membrane (13, 15, 16).

Cells harboring *nhx1*Δ mutations displayed a decrease in Na^+ tolerance only under specific conditions, such as acidic pH (pH 4.0) and low K^+ concentrations (1 mM) (12, 14). These data suggested the predominance of Na^+-ATPase and Nha1p over Nhx1p in Na^+ and K^+ tolerance and suggested other roles for Nhx1p. Nhx1p, also known as Vps44, act at the same step in trafficking to the vacuole as other class E vacuolar protein sorting proteins that are thought to control protein trafficking out of the pre-vacuolar compartment (17). Disruption of vacuolar the H^+-ATPase gene induced an increase of pH in the vacuolar lumen leading to a phenotype similar to that observed in *nhx1*Δ null mutants. This phenotype displayed changes in intravesicular activities and missorting of carboxypeptidase Y (17), suggesting that Nhx1p might play a role in regulating pH to control trafficking out of the endosome, inducing a H^+-leak that counterbalanced the action of the V-ATPase (16).

Contrary to a previous report (14), two independent studies showed that *nhx1* null mutants did not display reduced vacuolar Na^+ transport (18, 19) and that vacuolar preparations from different Na^+/H^+ antiporter yeast strain mutants, including KTA 40-2 (*ena1-ena4*Δ, *nha1*Δ, *nhx1*Δ, *kha1*Δ), did not display any reduction of Na^+ or K^+ transport.[2] These observations supported the notion that a vacuolar transporter, not encoded

[*]This work was supported by National Science Foundation Grant MCB-0343279. The costs of publication of this article were defrayed in part by the payment of page charges. This article must therefore be hereby marked "*advertisement*" in accordance with 18 U.S.C. Section 1734 solely to indicate this fact.

[1]To whom correspondence should be addressed: Dept. of Plant Sciences, Mail Stop 5, University of California, One Shields Ave., Davis, CA 95616. Tel.: 530-752-4640; Fax: 530-752-2278; E-mail:eblumwald@ucdavis.edu.

[2] O. Cagnac, unpublished data.

by the *NHX1* gene, could be responsible for the vacuolar cation/H^+ exchange activity seen in the yeast vacuoles (19). Because no other monovalent cation/H^+ homologues could be found in the databases, we decided to functionally screen a wide range of yeast cation/H^+ antiporter-like mutants from the Euroscarf collection to isolate the gene(s) coding the transporter responsible for the vacuolar cation/H^+ exchange activity. This reversed genetic approach allowed us to identify a single ORF[3] YNL321w, coding for a vacuolar Na^+ exchanger (Vnx1p). *vnx1*Δ mutants displayed a total loss of Na^+ and K^+/H^+ antiporter activity on vacuolar-enriched fraction.

Here we demonstrate that despite the high similarity of Vnx1p to the Ca^{2+}/H^+ antiporter Vcx1p, Vnx1p mediates vacuolar Na^+/H^+ and K^+/H^+ exchange and not Ca^{2+} transport. Expression of the *Arabidopsis* gene AtNHX1 in *vnx1*Δ cells restored the monovalent cation/H^+ exchange in isolated vacuoles, indicating that *vnx1*Δ mutants can provide a new tool for the heterologous expression and functional characterization of endosomal cation/H^+ antiporters.

EXPERIMENTAL PROCEDURES

Yeast Strains and Media—The *vnx1*Δ yeast strain (Table 1) was generated by replacing the *YNL321w* ORF with the kanMX6 gene by PCR-based gene deletion method (20) using the following primers: YNL31w-F1 (5′-AAGTGAAATAACTGCTAGCTAGAAGAGCGGTAAGCAGCACGGATCCCCGGGTTAATTAA-3′) and YNL31w-R1 (5′-AAAATTGGTAGGTATCCAGGTGAAAAGCGGGGAC AGTTGCGAATCGCTCGTTTAAAC-3′). The deletion constructs contain 40 bp of homology (underlined) to the beginning and to the end of the YNL321w ORF. Yeast strains were transformed by the deletion cassette using the standard lithium acetate method (21). Genomic DNA from Geneticin-resistant strains was isolated as described by Sambrook and Russell (22). Insertion of the disruption cassette into the correct locus was verified by PCR. Then, for each mutant strain three independent colonies were tested for their lack of vacuolar Na^+/H^+ and K^+/H^+ transport activity. All yeast strains used in this study are listed in Table 1. Yeast cells were grown in yeast 1% yeast extract, 2% peptone, 2% glucose or SD media (0.67% yeast nitrogen base, 2% glucose) with appropriate amino acid supplements as indicated.

Isolation of Intact Vacuoles from Yeast—Intact vacuoles were isolated as described by Ohsumi and Anraku (23). The intact vacuoles were collected at the top of the gradient and resuspended in 5 mM Tris-MES (pH 7.5). For vesicle preparation, 10% of glycerol and 1% of protease inhibitor mixture were added to resuspended vacuoles using a Dounce homogenizer. After centrifugation for 20 min at 100,000 × *g*, the vesicles were resuspended in 5 mM Tris-MES (pH 7.5). Protein concentrations were determined by the Bio-Rad DC protein assay according to the manufacturer's protocol.

Transport Assays—The fluorescence quenching of acridine orange was used to monitor the establishment and dissipation of vacuolar-inside acidic pH gradients as described before (24, 25). Intact vacuoles or vesicles (25 μg of protein) were used for each assay. Vacuoles were added to a buffer containing 50 mM tetramethyl ammonium chloride, 5 μM acridine orange, 5 mM Tris-MES (pH 7.5), and 3.125 mM $MgSO_4$. The vacuolar ATPase was activated by the addition of 5 mM Tris-ATP, and time-dependent fluorescence changes were monitored using a fluorescence spectrophotometer (PerkinElmer Life Sciences) with excitation and emission wavelengths of 495 and 540 nm, respectively, and a slit width of 5 nm with a 1% transmittance filter. When a steady-state pH gradient was established, the vacuolar ATPase was partially inhibited with the addition of 5–10 nM bafilomycin to obtain no net H^+ movements (*i.e.* equal rates of H^+ pump and H^+ leak (≈3 min) (see below); chloride salts were added as indicated. Initial rates were measured as the slope of the relaxation of the quench over a period of 30s. Rates were reported as % quench/min/mg of protein. All curves were normalized to 100% quench before quantification. Curves were fitted to the mean values of rates at each concentration measured by using KALEIDEGRAPH (Synergy Software, Reading, PA).

Plasmid Construction and Yeast Transformation—The yeast expression vector, pYOC003, used in this study is a modification of the pDR196 (26). 3 × Myc tag was amplified by PCR (Myc-For: 5′-CGCTCTGAGCAAAAGCTCA-3′ and Myc-Rev 5′-TCAGCGGCCGCTACTATT-3′) and then inserted in EcoRV of the pDR196 polylinker. The Gateway® cassette was amplified from the commercial vector pYES-DEST52 (Invitrogen) (attR1, 5′-ACAAGTTTGTACAAAAAAGCTG-3′; attR2, 5′-ACCACTTTGTACAAGAAAGC-3′) and then inserted in SmaI restriction site. The Vnx1 coding sequence (ORF: *YNL321w*) was cloned by PCR as describe in the Gateway® manual (Invitrogen) using the Expand high fidelity polymerase (Roche Applied Science). The PCR were performed on genomic DNA with primers attB1-Vnx1 (5′-GGGGACAAGTTTGTACAAAAAAGCAGGCTATGGCCAAAAATAACCACAT-3′) and attB2-Vnx1 (5′-GGGGACCACTTTGTACAAGAAAGCTGGGTCTACTCCGAAAGAGCTCCCT-3′). Homology to Gateway® recombination sites is underlined. For Vnx1–3xMyc fusion construct, attB1-Vnx1 primer was used in combination with attB2-Vnx1-Myc (5′-GGGGACCACTTTGTACAAGAAAGCTGGGTTCCGAAAGAGCTCCCTGGA-3′) primer. The resulting PCR product is a *VNX1* DNA sequence lacking the last four nucleotides, which allowed maintaining the same open reading frame between Vnx1 and 3 × Myc. The PCR products were cloned into the pDONR221 and pYOC003 using BP- and LR-Clonase MixII, respectively, as described by the manufacturer (Invitrogen).

Vnx1-GFP Localization—The *GFP* gene was inserted into the YNL321w ORF between the predicted transmembrane domain 7 and 8 by a PCR fusion-based method (27). *GFP6* without the stop codon was amplified by primers GFP-For (5′-ACGGTGCTAACGACCGTGACATGAGTAAAGGAGAAGAACT-3′) and GFP-Rev (5′-GGAGGATGCGAGAAAGTACAAGATCTTTTGTATAGTTCAT-3′). The underlined portion of the primers represents the homology to *VNX1*. The first part of YNL321w ORF (+1 to +1998) was amplified using primers attB1-Vnx1 (see above) and Vnx1-Rev (reverse complement of GFP-For), and the second part (+1999 to +2727) amplified

[3] The abbreviations used are: ORF, open reading frame; MES, 4-morpholineethanesulfonic acid; GFP, green fluorescent protein; ER, endoplasmic reticulum.

TABLE 1
List of strains used in this study

Strain	Genotype	Source
W303-1B	*Matα, ura3-1, leu2-3, trp1-1, his3-11,15, ade2-1, can1-100*	
KTA 40-2	*Matα, ura3-1, leu2-3, trp1-1, his3-11,15,ade2-1,can1-100, mal10, ena1–4Δ::HIS3, nhal Δ::LEU2, nhx1Δ::TRP1, tok1-khal Δ::KanMX*	Ref. 10
RGY296	*Matα, ura3-1, leu2-3, trp1-1, his3-11,15, can1-100, nhx1 Δ::HIS3*	Ref. 36
OC01	*Matα, ura3-1, leu2-3, trp1-1, his3-11,15, ade2-1, can1-100, ynl321w::KanMX2*	Euroscarf
OC02	*Matα, ura3-1, leu2-3, trp1-1, his3-11,15, can1-100, nhx1Δ::HIS3, ynl321w::KanMX4*	This study
RGY73	*Matα, ura3-1, leu2-3, trp1-1, his3-11,15, ade2-1, can1-100, ena1–2Δ::HIS3*	Ref. 36
OC03	*Matα, ura3-1, leu2-3, trp1-1, his3-11,15, ade2-1, can1-100, ena1–2Δ::HIS3, nhx1Δ::TRP1*	This study
OC04	*Matα, ura3-1, leu2-3, trp1-1, his3-11,15, ade2-1, can1-100, ena1–2Δ::HIS3, ynl321w::KanMX6*	This study
YJR106w	*Matα, ura3–52, his3Δ1, leu2-3_112, trp1-289, yjr106wΔ::HIS3*	Euroscraf
YDL128w	*Matα, ura3–52, trp1Δ63, vcx1Δ::kanMX4*	Euroscraf
YDL206w	*Matα, ura3–52, his3Δ200, trp1Δ63, ydl206wΔ::kanMX4*	Euroscraf
YLR220w	*Matα, his3Δ1, leu2Δ0, met15Δ0, ura3Δ0, ylr220w Δ::KanMX4*	Euroscraf
YOR316c	*Matα, his3Δ1, leu2Δ0, met15Δ0, ura3Δ0, yor316c Δ::KanMX4*	Euroscraf
YMR243c	*Matα, his3Δ1, leu2Δ0, met15Δ0, ura3Δ0, ymr243c Δ::KanMX4*	Euroscraf

using primers with attB2-Vnx1 (see above) and Vnx1-For (reverse complement of GFP-Rev) primers. All PCR products were combined and used as template for a nested PCR using attB1 and attB2 adaptors (5′-GGGGACAAGTTTGTACAAAAAGCAGGCT-3′; 5′-GGGGACCACTTTGTACAAGATGGGT-3′). Vnx1-GFP fused was cloned in a pYOC003 as previously described.

Growth Tests—Yeasts were grown in yeast extract/peptone/dextrose medium to saturation and washed twice in sterile water. All cell suspensions were adjusted to an optical density of 0.2, 0.02, and 0.002 in sterile water. 10 μl of each dilution were spotted onto yeast extract/peptone/dextrose media supplemented with 300 mM NaCl or 30 μg/ml hygromycin B. Growth was assessed at 30 °C after 2 days and 5 days for hygromycin B and NaCl, respectively.

Total Protein Extract and Western Blots—Yeast cells (A_{600} = 1) were washed and resuspended in water. To break the cells, the samples were incubated on ice for 10 min after the addition of 185 mM NaOH and 0.35% β-mercaptoethanol (0.35%). Total proteins were precipitated with 5% trichloroacetic acid on ice for 10 min. After centrifugation trichloroacetic acid-precipitated pellets were resuspended in 20 μl of 1 M Tris. Samples were denatured by adding an equivalent volume of 2× Laemmli buffer. Samples (20 μl) were subjected to a 6% SDS-PAGE followed by Western blot analysis. Anti-C-Myc-epitope monoclonal antibody (GeneTex, Inc. San Antonio, TX) and anti-mouse IgG antibody-horseradish peroxidase conjugate (Molecular Probes) were used at a dilution of 1:3,000 and 1:10,000, respectively.

Fluorescence Microscopy—A Leica DMR series fluorescent microscope equipped with a Chroma 86013 filter set (Chroma Technology, Rockingham, VT) and CoolSNAP-HQ (Roper Scientific, Tucson, AZ) was used to visualize the transformed cells. GFP was visualized by using filters S484/15 for excitation and S517/30 for emission. All images were taken at ×100 magnification. Images were pseudocolored with METAMORPH software (Universal Imaging, Downingtown, PA).

Gene Expression—Total RNA was isolated from yeasts with an RNeasy kit according to the manufacturer's protocol (Qiagen). Samples where then treated by DNase RNase-free (Roche Applied Science) to degrade the potential DNA contamination. Five micrograms of the total RNA were reverse then transcribed with iScript cDNA synthesis kit (Bio-Rad). PCR-specific primers to Nhx1 (forward, 5′-ACATGTCAAGAAGATCACAG 3′; reverse, 5′-TCGGCGTTGAGTAAGAGAGAATG-3′), to Vnx1 (forward, 5′-ATGGCCAAAAATAACCACAT-3′; reverse, 5′-ATTGGAACAAGTCACCTCCC-3′), and Kha1(forward, 5′-ATGGCAAACACTGTAGGAGG-3′; reverse, 5′-CAAATCGACATTTAATCCTGC-3′). One microliter of each cDNA sample was used to perform the gene specific PCR (35 cycles). The specificity of the PCR product was checked by sequencing.

RESULTS

Identification of YNL321w—A functional screening of yeast antiporter mutants from the Euroscarf collection was performed (Table 1). To select for putative vacuolar cation/H^+ antiporter-like proteins, we used the yeast transport protein data base (YTPdb) to choose only proteins that were predicted to be localized at the vacuole or at endosomes. Vacuoles were isolated from each of the Euroscarf knock-out mutants of putative cation/H^+ antiporters and knock-out mutants of the KHA1 encoding a putative K^+/H^+ antiporter and NHX1 encoding a pre-vacuolar-bound Na^+/H^+ antiporter (Table 1). The measurement of Na^+/H^+ and K^+/H^+ exchange activity in vacuoles isolated from each of the above-mentioned antiporters revealed insignificant changes to the transport (Na^+/H^+, K^+/H^+) seen in vacuoles isolated from wild-type yeast (Fig. 1, *A–C*), with exception of *ynl321Δ* (Fig. 2*B*). Vacuoles isolated from the YNL321w ORF knock-out showed the absence of a cation/H^+ exchange activity (Fig. 2*B*). To further confirm YNL321 function(s), the transport activity of *ynl321Δ* knock-outs that were complemented with the *YNL321* gene was studied. VNX1 was cloned into a high expression vector downstream of the PMA1 promoter. Transformation of the *ynl321Δ* disruptants with this construct restored Na^+/H^+, K^+/H^+, and Li^+/H^+ transport of the vacuoles (Fig. 2*C*), confirming YNL321 as a monovalent cation/H^+ antiporter.

The cation/H^+ transport activity of YNL321 was dependent on the pH gradient generated by the vacuolar H^+-ATPase. It should be noted that a steady-state ΔpH gradient without net H^+ movements was established after the addition of a relatively low bafilomycin A concentration (10 nM) that partially inhibited the H^+-ATPase. Further inhibition of the H^+-ATPase with increasing concentrations of bafilomycin A increased the H^+ conductance of the vacuoles, thus impinging on the measurements of cation-dependent H^+ movements mediated by YNL321 (Fig. 2*D*). The addition of 1 μM bafilomycin before the addition of ATP totally abolished the formation pH gradient.

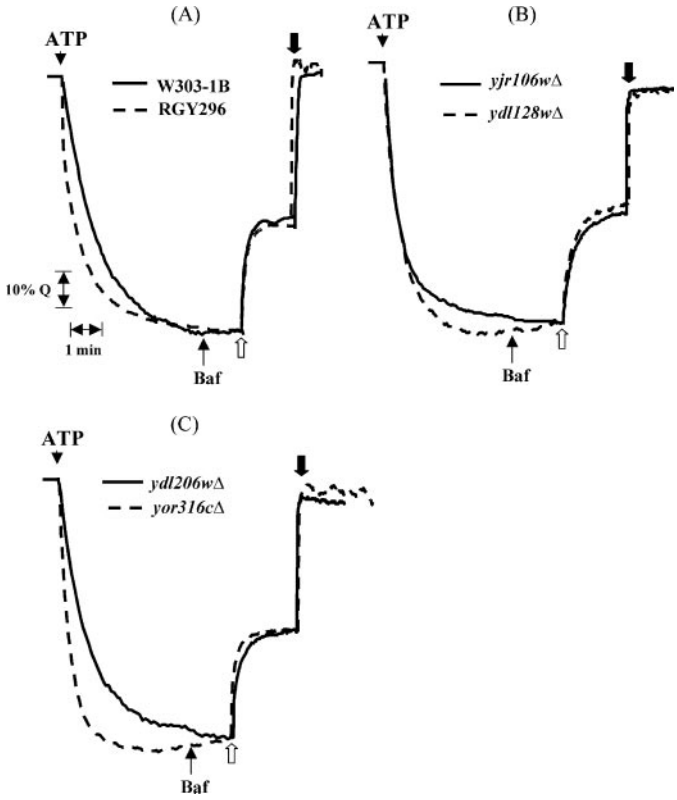

FIGURE 1. **Vacuolar cation-dependent H^+ transport.** Cation-dependent proton movements were monitored by following the fluorescence quenching of acridine orange as described under "Experimental Procedures." At the indicated times vesicle acidification was initiated by the addition of ATP. After a steady-state acidic-inside pH gradient was attained, the activity of the H^+-ATPase was partially inhibited by the addition of 10 nM bafilomycin (*Baf*). At the indicated times (*white arrows*) 50 mM KCl was added, resulting in a cation-dependent H^+ movement and the alkalinization of the vesicular lumen (recovery of the fluorescence). At the indicated times (*black arrows*) 5 μM nigericin was added to collapse the ΔpH across the tonoplast. Assays were performed with various yeast strains as indicated (*A*, *B*, and *C*).

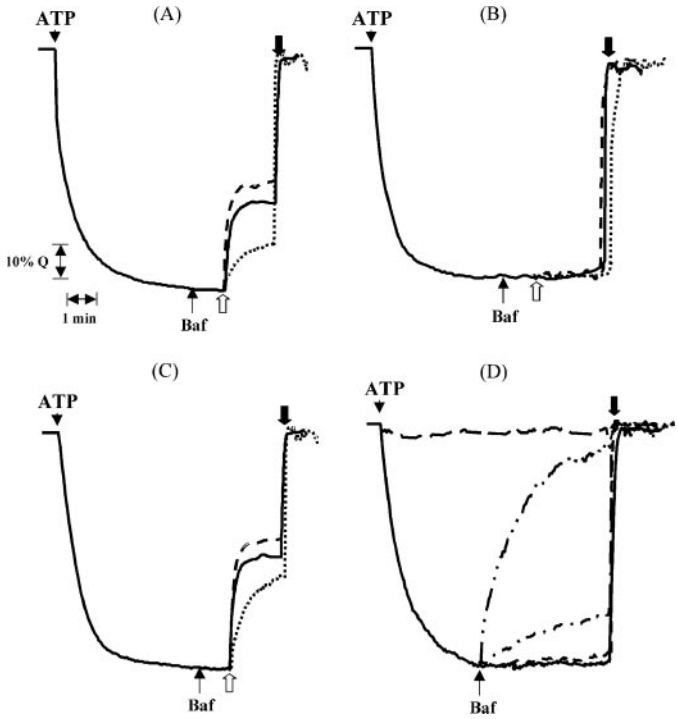

FIGURE 2. **Vacuolar cation-dependent H^+ transport.** Cation-dependent proton movements were monitored by following the fluorescence quenching of acridine orange as described under "Experimental Procedures." At the indicated times vesicle acidification was initiated by the addition of ATP. After a steady-state acidic-inside pH gradient was attained, the activity of the H^+-ATPase was partially inhibited by the addition of 10 nM bafilomycin (*Baf*). At the indicated times (*white arrows*) 50 mM NaCl (– – – – –), 50 mM KCl (——), or 50 mM LiC (. . . . . .) were added, resulting in a cation-dependent H^+ movement and the alkalinization of the vesicular lumen (recovery of the fluorescence). At the indicated times (*black arrows*) 5 μM nigericin (for K^+) or 5 μM monensin (for Na^+ or Li^+) were added to collapse the ΔpH across the tonoplast. *A*, assays were performed with wild-type yeast strain. *B*, vnx1Δ cells. *C*, vnx1Δ complemented with *VNX1*. *D*, inhibition of V-ATPase activity by bafilomycin A. Bafilomycin A 10 nM (– – – – –), 30 nM (—·—·—), or 100 nM (—··—··—) was added where indicated (*Baf*). One μM bafilomycin A (———) was added before ATPase activation. (after a steady-state pH gradient was obtained of specific inhibitor bafilomycin A (*D*). Traces are representative of at least 5 independent experiments.

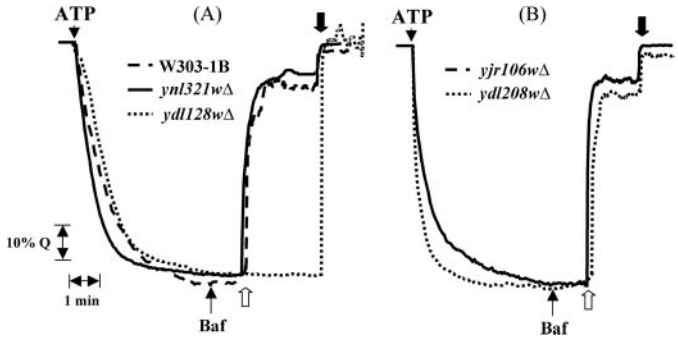

FIGURE 3. **Cation-dependent H^+ transport in across vacuolar vesicles.** Proton movements were monitored by following the fluorescence quenching of acridine orange as described under "Experimental Procedures" and Fig. 1. At the indicated times 10 nM bafilomycin (*Baf*) and 6.25 μM $CaCl_2$ (*white arrows*) and 5 μM nigericin plus 5 mM KCl were added. Assays were performed with different mutants of the Vcx family: (*A*) *ynl321wΔ*, *ydl128w* (*vcx1Δ*), the wild-type (W303-1B); (*B*) *yjr106wΔ* and *ydl208wΔ*. Traces are representative of at least three independent experiments.

Noteworthy, from the members of the yeast Vcx family (comprising YDL128w, YDL206w, YJL106w, and YNL321w), only YDL128w, encoding Vcx1p, has been shown to mediate vacuolar Ca^{2+}/H^+ exchange antiporters (28). Vacuoles of YNL321w displayed Ca^{2+}/H^+ exchange activity that was comparable with that of vacuoles isolated from wild-type yeast (strain W303-1B). Nevertheless, the vacuolar Ca^{2+}/H^+ exchange activity was completely abolished in vacuoles isolated from *vcx1Δ* cells (Fig. 3), indicating that the Ca^{2+}/H^+ exchange was mediated exclusively by Vcx1p, as demonstrated by Pozos *et al.* (28), and that YNL321w did not contributed to this activity. Our results show that despite its inclusion in the VCX family by the YTP data base, YNL321w transports monovalent and not divalent cations.

Sequence Analysis of YNL321W—The deduced amino acid sequence indicated that the *YNL321* encodes a 908-amino acid polypeptide with a pI of 7.13 and a predicted molecular mass of 102.498 kDa that is very similar to the 106 kDa revealed by immunodetection of the Myc-tagged YNL321w (Fig. 4*C*). Analysis of the hydropathy profile suggests the presence of 13 putative transmembrane domains and a 242-amino-acid-long hydrophilic N terminus (Fig. 4*A*). YNL321w belongs to the CAX (calcium exchanger) family, that together with YRBG, NCX, NCKX, and CCX families form the cation/Ca^{2+} exchanger superfamily (29). We compared the protein sequence of YNL321w with other mem-

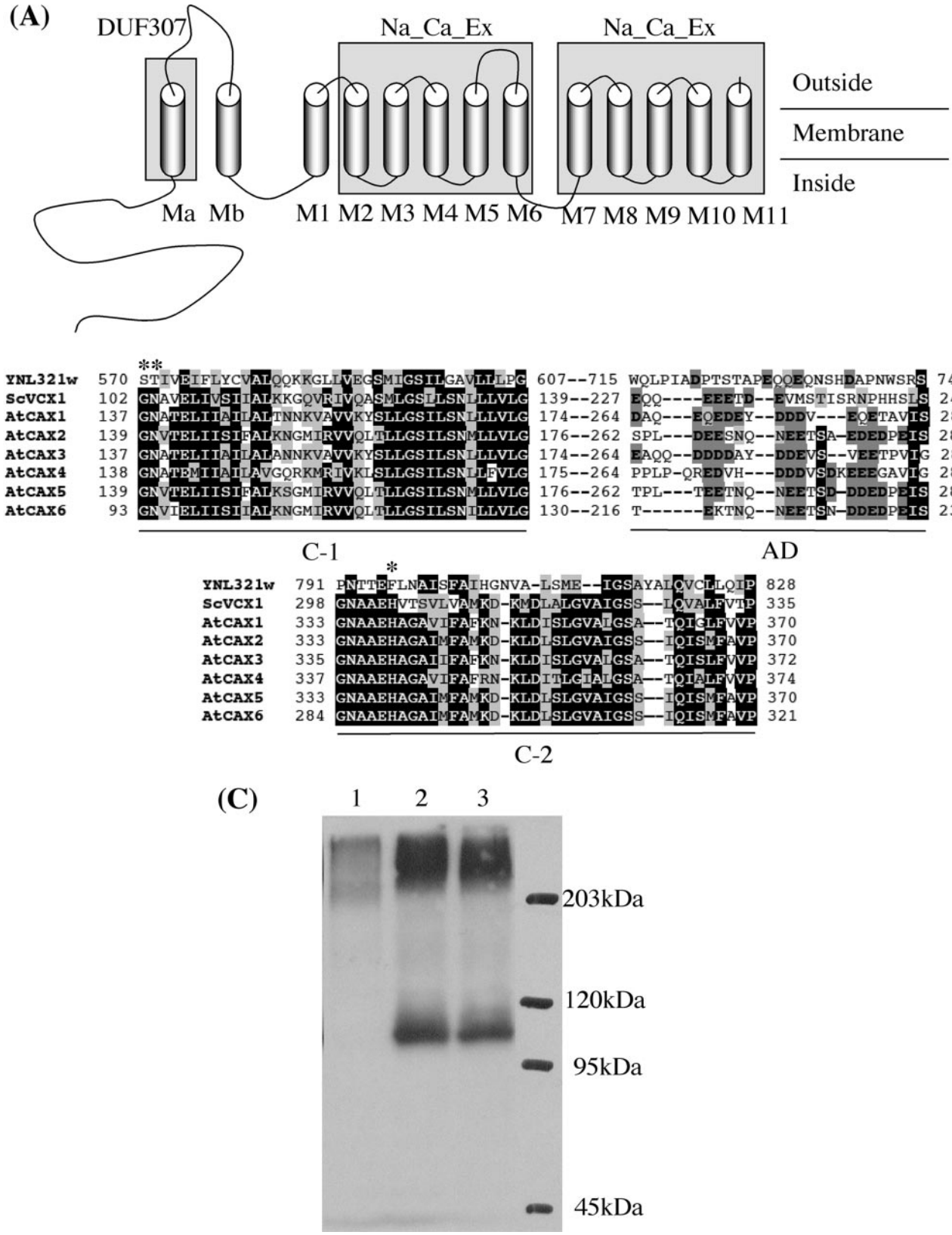

FIGURE 4. **Sequence analysis of YNL321W.** *A*, topological model based on predictions using TMHMM 2.0 program (49). M1–M11 indicate the 11 transmembrane domains similar to other CAXs; Ma and Mb are the two additional transmembrane domains found in the first half of the protein. The *gray squares* represent the conserved domains (DUF307 and Na_Ca_Ex) identified by Pfam. *B*, alignment of deduced amino acid sequences of YNL321W (M1–11), ScVCX1. and type-I CAXs from *A. thaliana*. Alignments were performed using ClustalW in the MEGA3 program, Consensus amino acid residues are boxed in *black* (identical) or *light gray* (similar). In the acidic domain (*AD*), acidic residues are represented by bold-faced letters and *dark gray boxes*. Residues important for calcium transport are indicated by *stars*. *C*, immunodetection of c-Myc-tagged YNL321w. Shown are proteins isolated from W303 transformed with empty plasmid (*1*), W303 expressing c-Myc-tagged YNL321w (*2*), and *ynl 321w*Δ cells expressing c-Myc-tagged YNL321w (*3*).

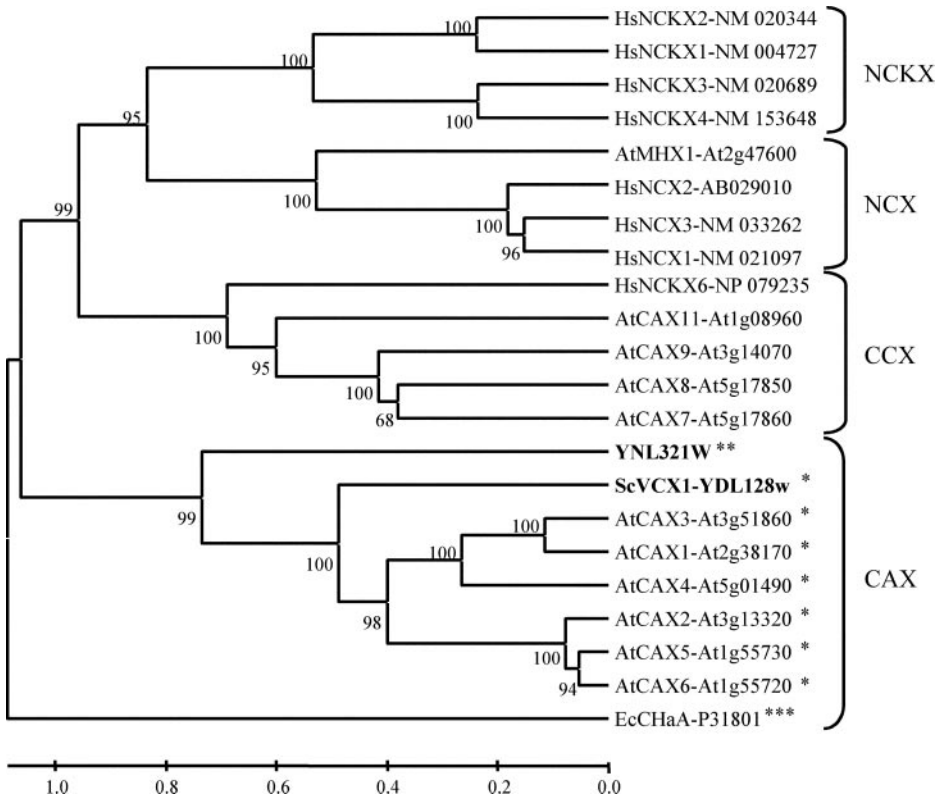

FIGURE 5. **Phylogenetic tree of cation/Ca^{2+} exchanger superfamily members of *S. cerevisiae* (*Sc*), *A. thaliana* (*At*), *Homo sapiens* (*Hs*), and *Escherichia coli* (*Ec*).** Appurtenance to one of the three subgroup of CAX family is symbolized by the presence of *one*, *two*, or *three stars* after the name. The tree was inferred with MEGA3 using the UPGMA method. *Numbers* indicated at the branch nodes are the bootstrap values from 1000 replicates.

bers of this superfamily (Fig. 5). The closest homolog to YNL321W is ScVCX1, a *S. cerevisiae* vacuolar Ca^{2+}/H^+ antiporter (30). Despite their similarity, ScVCX1 and YNL321W belong to two distinct groups of the CAX family (31). *Sc*VCX1 and the *Arabidopsis thaliana At*CAX1–6 form the type I of CAX antiporters, whereas YNL321W belongs to the type II of CAXs that are only present in fungi, *Dictyostelium*, and lower vertebrates. YNL321W contains some of the special structural features characteristic of the type II CAXs (31); (i) the first half of its protein sequence (amino acids 1–524) contains a conserved domain of unknown function, DUF307, and two predicted transmembrane domains (Fig. 4*A*); (ii) the second half of the protein (amino acids 525–908) is highly similar to the type I CAXs with 11 predicted transmembrane domains and the conserved domain Na_Ca exchanger (pfam PF01699) repeated twice, as in all the members of the cation/Ca^{2+} exchanger superfamily. However, YNL321W has some unique features. First, the acidic motif, a stretch of negatively charged amino acids in the loop between the two Na_Ca_Ex conserved domains (32), is absent in YNL321W (Fig. 4*B*). This acidic motif, found in several Ca^{2+}-binding proteins such as calsequestrin, calreticulin, and the cation/Ca^{2+} exchangers, is believed to be indicative of Ca^{2+} transport activity (32). Moreover, several amino acid residues (marked with the *asterisk* in Fig. 4*B*) that were identified as crucial for calcium transport in CAXs from *Arabidopsis* (*i.e.* Leu-87, Gly-137, Asn-138, and His-338) and rice are different in YNL321W. These residues in regions named c-1 and c-2 in the CAX family are highly conserved (33), and mutations at some of these specific sites induced loss of Ca^{2+} transport activity (34).

Functional Characterization—Altogether, the transport data and sequence analysis strongly suggested that the protein encoded by *YNL321w* is a tonoplast-bound monovalent cation/H^+ antiporter. We could not designate the *YNL321w* ORF Vcx (c for cation), this name being already attributed to vacuolar H^+/Ca^{2+} exchanger 1 or Nhx (Na^+/h^+ exchanger) due to the lack of similarity between YNL321w and NHX1p. Therefore, we termed YNL321w vacuolar Na^+/H^+ exchanger 1 (Vnx1).

To characterize the kinetic characteristics of cation/H^+ exchange mediated by Vnx1p, we used the wild-type strain. Given that the disruption of *VNX1* induced the total loss of vacuolar cation/H^+ exchange activity, then the measurement of this activity in vacuoles of the wild-type strain (W303-1B) would represent the Vnx1p activity. Our assumptions are only valid if the contribution of other tonoplast-bound cation/H^+ antiporters is minimal. The only other endosomal cation/H^+ antiporter that could contribute to monovalent cation/H^+ exchange in the vacuole is Nhx1p. Nhx1p, a pre-vacuolar cation/H^+ antiporter, has been extensively characterized (13, 15). Nhx1p appears to be localized at the pre-vacuolar compartment and possibly to the vacuole. Nevertheless in our experimental conditions Nhx1p activity was not detected in vacuoles isolated from *vnx1*Δ, and vacuoles isolated from *nhx1* mutant strains were not impaired in Na^+/H^+ or K^+/H^+ activity (results not shown). Similar results were also reported elsewhere (18, 19). Vacuolar Nhx1p-driven cation/H^+ exchange was only detected when its expression was driven by the strong promoter PMA1 (Fig. 6*A*). These observations confirmed our assumptions that Vnx1p is responsible for the cation/H^+ exchange in our vacuolar preparations. Our findings showing that vacuoles isolated from *S. cerevisiae vnx1*Δ lack monovalent cation/H^+ exchange activity provides a powerful tool for the study of heterologous monovalent cation/H^+ antiporters. For example, vacuoles isolated from *S. cerevisiae vnx1*Δ cells expressing *AtNHX1* displayed cation/H^+ exchange activity mediated by the plant antiporter (Fig. 6*B*).

The transport activity of Vnx1p was further characterized using vacuoles isolated from the wild-type strain (W303-1B) as well as the *vnx1*Δ strain as a control. A vacuolar acidic-inside

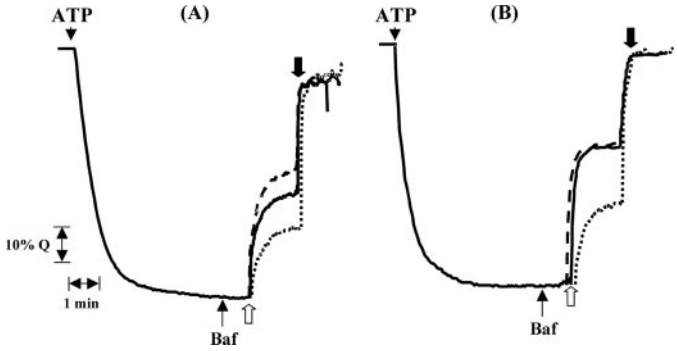

FIGURE 6. **Expression of monovalent cation/H$^+$ antiporters in *vnx1*Δ cells.** Proton movements were monitored by following the fluorescence quenching of acridine orange as described under "Experimental Procedures" and Fig. 1. At the indicated times (*white arrows*) 50 mM NaCl (–––––), 50 mM KCl (——), or 50 mM LiC (. . . . . .) were added to collapse the ΔpH across the tonoplast, resulting in a cation-dependent H$^+$ movement and the alkalinization of the vesicular lumen (recovery of the fluorescence). At the indicated times (*black arrows*) 5 μM nigericin (for K$^+$) or 5 μM monensin (for Na$^+$ or Li$^+$) were added to collapse the ΔpH across the tonoplast. Assays were performed with *vnx1*Δ cells over expressing *NHX1* (*A*) or *AtNHX1* (*B*). *Baf*, bafilomycin.

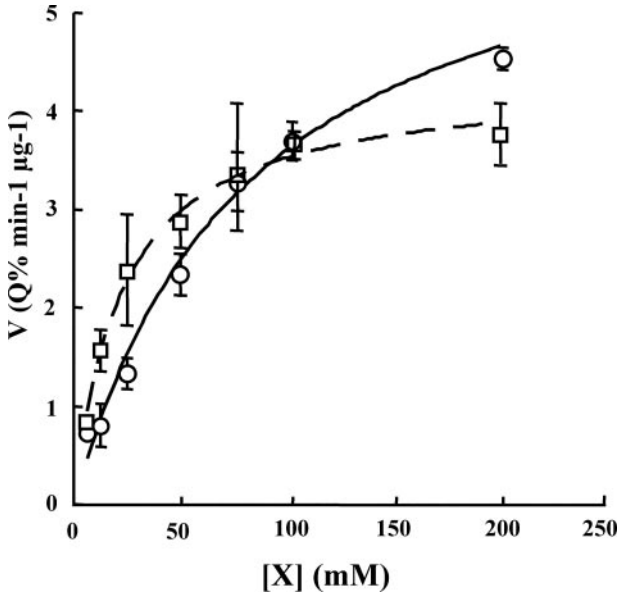

FIGURE 7. **Vnx1p-mediated cation/H$^+$ exchange kinetics.** Initial rates of cation-dependent H$^+$ movement were assayed by measuring the initial rates of fluorescence quench recovery after the addition of NaCl or KCl as described under "Experimental Procedures." *Solid lines* with *filled circles* are *fitted curves* for rates of K$^+$ transport, whereas *dashed lines* with *open filled squares* are fitted curves for Na$^+$ transport. Each data point is the mean ± S.D. (n = 3).

pH was generated by the activation of the V-type H$^+$-ATPase as described under "Experimental Procedures." Once a steady-state pH difference was attained, the H$^+$ pump activity was stopped by the addition of the specific inhibitor bafilomycin A (35), and the initial rates of cation (Na$^+$, K$^+$ or Li$^+$)-dependent H$^+$ movements were measured. The cation-dependent H$^+$ fluxes displayed a Michaelis-Menten-type saturation kinetics (Fig. 7) with apparent K_m of 22.4 ± 2.5 and 82.2 ± 16 mM for Na$^+$ and K$^+$, respectively.

*Growth Comparison of vnx1*Δ *and nhx1*Δ *Mutant*—Because of the apparent functional similarity between Nhx1p and Vnx1p, we compared the sensitivities of *vnx1*Δ and *nhx1*Δ mutant strains to hygromycin B and alkali salts (Fig. 8). It was shown previously that yeast lacking genes encoding Nhx1p displayed sensitivity to hygromycin B (36). The high sensitivity of *nhx1*Δ cells to hygromycin B appears to be due to a defective sequestration of toxic cations into intracellular compartments (37), and the mechanism by which Nhx1p confers tolerance to hygromycin B appears to be associated with the role of Nhx1p in intravesicular pH regulation (16). *vnx1*Δ cells also displayed sensitivity to hygromycin B, and the disruption of VNX1 in the nhx1Δ strain resulted in the total growth inhibition of the double mutant *nhx1*Δ *vnx1*Δ cells. No growth defect was observed in the single mutant *nhx1*Δ or *vnx1*Δ cells in the presence of increasing concentrations of NaCl (results not shown). Because of the dominant role of the plasma membrane-bound Na$^+$-ATPases in Na$^+$ extrusion in *S. cerevisiae* (5), we generated *vnx1*Δ mutants based on W303 1-B *ena1-ena4*Δ sodium sensitive strain and tested the tolerance of the double mutant to NaCl and LiCl. To minimize the effect of plasma membrane-bound Nha1p in the extrusion process, the drop tests were performed at neutral rather than acidic pH (5). After 5 days of incubation at 30 °C in the presence of NaCl, the growth of *vnx1*Δ and *nhx1*Δ disruptants was inhibited similarly, whereas LiCl had a much more inhibitory effect on *nhx1*Δ than on *vnx1*Δ cells. Reverse transcription-PCR showed that the expression of VNX1 correlated well with the respective phenotypes (Fig. 8*C*). These results would indicate that although Ena1-Ena4 are the main contributors to Na$^+$ homeostasis in *S. cerevisiae*, there is a contribution of Vnx1p mediating Na$^+$ (and Li$^+$) transport into the yeast vacuole.

GFP Localization—The cation/H$^+$ exchange activity mediated by Vnx1p in isolated vacuoles and tonoplast vesicles and the dependence of Vnx1p activity on the proton gradients built by the V-ATPase (sensitive to bafilomycin A) indicated the vacuolar localization of Vnx1p (Fig. 2). In absence of available antibodies raised against Vnx1p, we expressed the chimera Vnx1p::GFP with the GFP fused at the C terminus of Vnx1p. Under these conditions Vnx1p-GFP fluorescence was detected in the endoplasmic reticulum (ER) (Fig. 9, *A* and *B*). This observation was confirmed by the fluorescence of Erg1-GFP, a specific marker of the ER and lipid droplets (38) (Fig. 9, *C* and *D*). It has been shown previously that C terminus-tagged proteins can remain trapped in the ER (39), since the presence of a tag (GFP or Myc) at the C terminus often leads to the misfolding of the protein, its retention in the ER, and eventually its degradation by the ER-associated degradation machinery (40). A data base of the global analysis of protein localization in *S. cerevisiae* using GFP::C terminus-tagged proteins (41) showed that Vcx1p, a known vacuolar cation/proton antiporter, remained trapped in the ER. Similar results were reported when Nhx1p-HA was overexpressed using a 2-μm plasmid using the endogenous *NHX1* promoter (17) A search in the data base for other vacuolar GFP-tagged proteins showed a partial or full retention of the protein in the ER compartment. Froissard *et al.* (39) showed that when the tag was introduced inside a central loop of the transport protein, the ER retention was only partial. We constructed a new chimeric gene encoding Vnx1p with a GFP fused to the hydro-

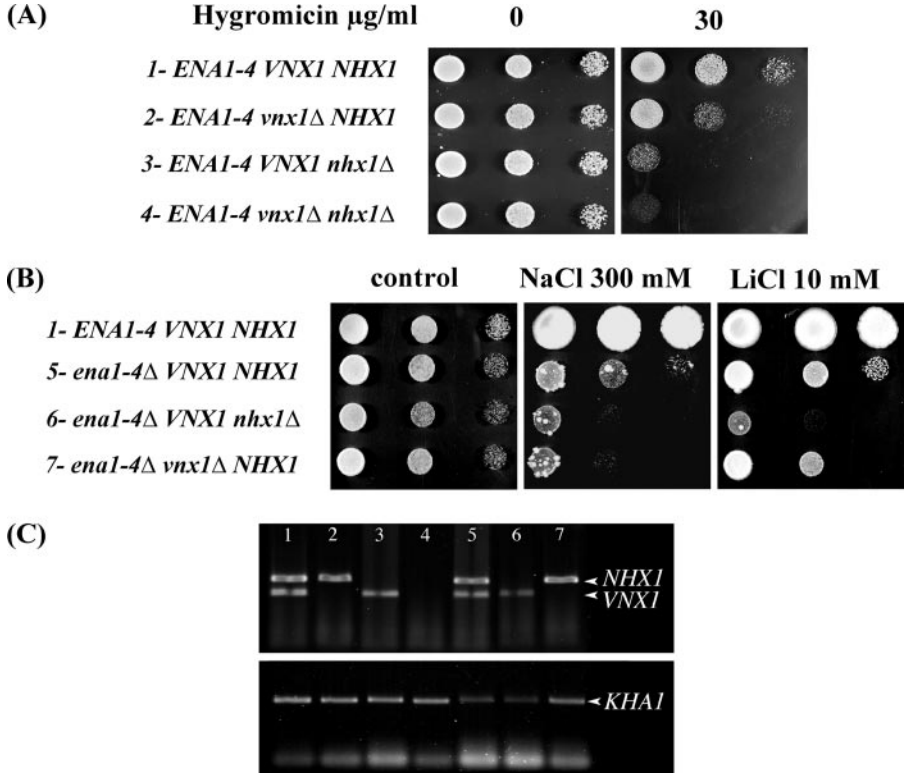

FIGURE 8. **Growth of *vnx1* mutants in the presence of toxic cations and *VNX1* expression.** Serial dilutions of the indicated strains were incubated at 30 °C for 2 days in the presence of hygromycin B (*A*) and 5 days in the presence of NaCl or LiCl (*B*). Control plates were grown for 1 day. *C*, *VNX1* expression in the different yeast strains. Reverse transcription-PCR was performed as described under "Experimental Procedures." *Numbers* indicate strains used in *A* and *B*.

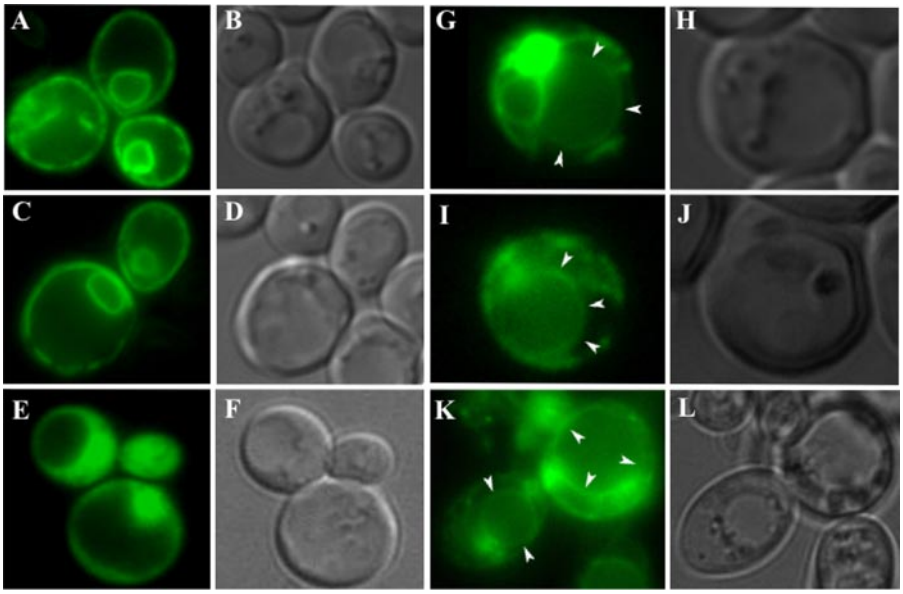

FIGURE 9. **Vacuolar localization of Vnhx1p.** *A*, yeast cells expressing *VNX1::GFP* inserted at the C terminus. *C*, yeast cells expressing the ER marker ERG1::GFP. *E*, yeast cells expressing GFP alone. *G*, *I*, and *K*, yeast cells expressing *VNX1::GFP* inserted between predicted transmembrane domains 7 and 8 (*B*, *D*, *F*, *H*, *J*, and *L*) Corresponding contrasted images of yeast cells are shown. Images were acquired as described under "Experimental Procedures." *Arrows* indicate vacuolar membrane.

philic loop between the predicted transmembrane domains 7 and 8. Our results showed that although there was an ER signal, indicative of a partial retention of the protein, a vacuolar signal of *Vnx1::GFP* was detected (Fig. 9, *G–L*). When GFP was expressed alone, the typical fluorescence in the cytosol was seen (Fig. 9, *E* and *F*).

DISCUSSION

To date, several transport systems operating to maintain monovalent cation homeostasis in *S. cerevisiae* have been characterized. At the plasma membrane, a Na^+-ATPase (Ena1-Ena4) and a cation/H^+ antiporter (Nha1p) mediate Na^+ extrusion out of the cell (4, 5, 42). A pre-vacuolar-bound Na^+/H^+ antiporter (Nhx1p) mediates cation/H^+ exchange in prevacuoles and possibly in other intracellular compartments (12, 16). More recently, a K^+/H^+ exchanger (Kha1p) at the Golgi was reported, and its role in pH regulation was postulated (10, 11). Although in *S. cerevisiae*, vacuolar Na^+ (and K^+) transport has been attributed mainly to Nhx1p (14), our data and other reports (18, 19) support the notion that Nhx1p is not involved in vacuolar Na^+/H^+ exchange and that another transporter is involved in vacuolar monovalent cation homeostasis.

Our strategy, the measurements of cation/H^+ exchange activities of all of the knock-out mutants lacking putative cation/H^+ antiporters, allowed us to identify Vnx1p, a novel vacuolar monovalent cation/H^+ antiporter, and to functionally characterize its activity. The loss of monovalent cation/H^+ exchange in vacuoles isolated form *vnx1* mutants, the restoration of the transport activity upon complementation of the *vnx1*Δ mutant with a plasmid bearing *VNX1*, and the localization of Vnx1p to the vacuole provided evidence that *VNX1* encodes a vacuolar monovalent cation/H^+ antiporter. Vnx1p belongs to the cation exchanger family (CAX), known to mediate Ca^{2+}/H^+ exchange (31). Our work is the first to identify and functionally characterize a type II CAX transporter, showing that Vnx1p does not transport Ca^{2+} ions. Interestingly, the lack of Ca^{2+} transport is correlated with the absence of key amino acids shown to be essential for Ca^{2+} transport in other CAXs members (33, 34).

Our results clearly indicated that Vnx1 mediated Na^+, K^+, and Li^+ transport into the vacuole and that the lack of Vnx1p increased the salt sensitivity of the cells. Nevertheless, similar to what was shown for *nha1*Δ and *nhx1*Δ strains (37), the growth of *vnx1*Δ single mutants in the presence of 300 mM NaCl or 10 mM LiCl was not affected. On the other hand, the growth of the *ena1-ena4*Δ *vnx1*Δ cells was affected in the presence of either NaCl or LiC, thus indicating the predominant role of Ena1-Ena4 in Na^+ extrusion. *S. cerevisiae* is able to accumulate different ions in the cell to up to 3–30 times the external concentration, but Na^+ are largely excluded, with cells showing only 30% of the Na^+ concentration of the growth medium (43). Moreover, ionomic analysis of *nhx1*Δ and *nha1*Δ cells failed to show any significant differences in ion content relative to wild type, reinforcing the notion that Na^+-ATPases are predominant in *S. cerevisiae* Na^+ homeostasis. *vnx1*Δ cells displayed sensitivity to hygromycin B, and the growth of the double mutant *nhx1*Δ *vnx1*Δ was halted by hygromycin B, suggesting that, similar to the role of Nhx1p in the pre-vacuolar compartment (16), Vnx1p is also involved in the regulation of the intravacuolar pH regulation.

Although speculative, the potential involvement of Vnx1p in cell division has been postulated (44). Vnx1p was found to be the substrate of the Cdc28p/Clb2p enzymatic complex, and a number of cyclin-dependent kinase consensus phosphorylation sites (45, 46) have been identified in the Vnhx1p N-terminus (44). In addition, *VNX1* expression was dramatically inhibited (log 2 ratio of −6.64) when cells were exposed to α-factor (47), a pheromone that stimulates yeast cells to increase the expression of mating genes and arrest cell division in the G_1 phase of the cell cycle (48).

In conclusion, we have analyzed all the of the knockouts of *S. cerevisiae* lacking monovalent and divalent cation/H^+ antiporters to identify the vacuolar monovalent cation/H^+ antiporter that mediates the H^+-coupled transport of Na^+, K^+, and Li^+ in *S. cerevisiae* vacuoles. We identified Vnx1p, a novel cation/H^+ transporter encoded by YNL321w. Although YNL321w belongs to the Vcx family of putative type-II vacuolar Ca^{2+}/H^+ exchangers and contrary to what it has been assumed till now, Vnx1p only mediates the transport of monovalent and not divalent cations. Vnx1p is a low affinity cation/H^+ antiporter with higher affinity for Na^+ than for K^+. The vacuolar-bound Vnx1p appears to play roles in ion homeostasis and intracellular pH regulation, similar to the prevacuolar-bound Nhx1p. Because of its predominant role in vacuolar ion transport, *vnx1*Δ mutant cells can provide a new and important tool of the heterologous expression and functional characterization of endosomal monovalent cation/H^+ antiporters.

Acknowledgment—We thank Sebastien Leon for help.

REFERENCES

1. Gaber, R. F., Styles, C. A., and Fink, G. R. (1988) *Mol. Cell. Biol.* **8,** 2848–2859
2. Ko, C. H., Buckley, A. M., and Gaber, R. F. (1990) *Genetics* **125,** 305–312
3. Michel, B., Lozano, C., Rodriguez, M., Coria, R., Ramirez, J., and Pena, A. (2006) *Yeast* **23,** 581–589
4. Haro, R., Garciadeblas, B., and Rodriguez-Navarro, A. (1991) *FEBS Lett.* **291,** 189–191
5. Prior, C., Potier, S., Souciet, J. L., and Sychrova, H. (1996) *FEBS Lett.* **387,** 89–93
6. Simon, E., Clotet, J., Calero, F., Ramos, J., and Arino, J. (2001) *J. Biol. Chem.* **276,** 29740–29747
7. Ohgaki, R., Nakamura, N., Mitsui, K., and Kanazawa, H. (2005) *Biochim. Biophys. Acta* **1712,** 185–196
8. Padan, E., Venturi, M., Gerchman, Y., and Dover, N. (2001) *Biochim. Biophys. Acta* **1505,** 144–157
9. Banuelos, M. A., and Rodriguez-Navarro, A. (1998) *J. Biol. Chem.* **273,** 1640–1646
10. Maresova, L., and Sychrova, H. (2005) *Mol. Microbiol.* **55,** 588–600
11. Flis, K., Hinzpeter, A., Edelman, A., and Kurlandzka, A. (2005) *Biochem. J.* **390,** 655–664
12. Nass, R., Cunningham, K. W., and Rao, R. (1997) *J. Biol. Chem.* **272,** 26145–26152
13. Nass, R., and Rao, R. (1998) *J. Biol. Chem.* **273,** 21054–21060
14. Darley, C. P., van Wuytswinkel, O. C. M., van der Woude, K., Mager, W. H., and de Boer, A. H. (2000) *Biochem. J.* **351,** 241–249
15. Nass, R., and Rao, R. (1999) *Microbiology* **145,** 3221–3228
16. Brett, C. L., Tukaye, D. N., Mukherjee, S., and Rao, R. (2005) *Mol. Biol. Cell* **16,** 1396–1405
17. Bowers, K., Levi, B. P., Patel, F. I., and Stevens, T. H. (2000) *Mol. Biol. Cell* **11,** 4277–4294
18. Hirata, T., Wada, Y., and Futai, M. (2002) *J. Biochem.* (*Tokyo*) **131,** 261–265
19. Martinez-Munoz, G. A., and Pena, A. (2005) *Yeast* **22,** 689–704
20. Longtine, M. S., McKenzie, A., III, Demarini, D. J., Shah, N. G., Wach, A., Brachat, A., Philippsen, P., and Pringle, J. R. (1998) *Yeast* **14,** 953–961
21. Gietz, R. D., Schiestl, R. H., Willems, A. R., and Woods, R. A. (1995) *Yeast* **11,** 355–360
22. Sambrook, J., and Russell, D. W. (2001) *Molecular Cloning: A Laboratory Manual*, Cold Spring Harbor Laboratory Press, Cold Spring Harbor, New York
23. Ohsumi, Y., and Anraku, Y. (1981) *J. Biol. Chem.* **256,** 2079–2082
24. Blumwald, E., Rea, P. A., and Poole, R. J. (1987) *Methods Enzymol* **148,** 115–123
25. Yamaguchi, T., Apse, M. P., Shi, H., and Blumwald, E. (2003) *Proc. Natl. Acad. Sci. U. S. A.* **100,** 12510–12515
26. Wipf, D., Benjdia, M., Rikirsch, E., Zimmermann, S., Tegeder, M., and Frommer, W. B. (2003) *Genome* **46,** 177–181
27. Hobert, O. (2002) *Biotechniques* **32,** 728–730
28. Pozos, T. C., Sekler, I., and Cyert, M. S. (1996) *Mol. Cell. Biol.* **16,** 3730–3741
29. Cai, X. J., and Lytton, J. (2004) *Mol. Biol. Evol.* **21,** 1692–1703
30. Cunningham, K. W., and Fink, G. R. (1996) *Mol. Cell. Biol.* **16,** 2226–2237
31. Shigaki, T., Rees, I., Nakhleh, L., and Hirschi, K. D. (2006) *J. Mol. Evol.* **63,** 815–825
32. Ivey, D. M., Guffanti, A. A., Zemsky, J., Pinner, E., Karpel, R., Padan, E., Schuldiner, S., and Krulwich, T. A. (1993) *J. Biol. Chem.* **268,** 11296–11303
33. Kamiya, T., and Maeshima, M. (2004) *J. Biol. Chem.* **279,** 812–819
34. Shigaki, T., Barkla, B. J., Miranda-Vergara, M. C., Zhao, J., Pantoja, O., and Hirschi, K. D. (2005) *J. Biol. Chem.* **280,** 30136–30142
35. Bowman, E. J., Siebers, A., and Altendorf, K. (1988) *Proc. Natl. Acad. Sci. U. S. A.* **85,** 7972–7976
36. Gaxiola, R. A., Rao, R., Sherman, A., Grisafi, P., Alper, S. L., and Fink, G. R. (1999) *Proc. Natl. Acad. Sci. U. S. A.* **96,** 1480–1485
37. Kinclova-Zimmermannova, O., Gaskova, D., and Sychrova, H. (2006) *FEMS Yeast Res.* **6,** 792–800
38. Leber, R., Landl, K., Zinser, E., Ahorn, H., Spok, A., Kohlwein, S. D., Turnowsky, F., and Daum, G. (1998) *Mol. Biol. Cell* **9,** 375–386
39. Froissard, M., Belgareh-Touzé, N., Buisson, N., Desimone, M., Frommer, W., and Haguenauer-Tsapis, R. (2006) *Biotechnol. J.* **1,** 308–320
40. Ahner, A., and Brodsky, J. L. (2004) *Trends Cell Biol.* **14,** 474–478
41. Huh, W. K., Falvo, J. V., Gerke, L. C., Carroll, A. S., Howson, R. W., Weissman, J. S., and O'Shea, E. K. (2003) *Nature* **425,** 686–691
42. Banuelos, M. A., Sychrova, H., Bleykasten-Grosshans, C., Souciet, J. L., and Potier, S. (1998) *Microbiology* **144,** 2749–2758

43. Eide, D. J., Clark, S., Nair, T. M., Gehl, M., Gribskov, M., Guerinot, M. L., and Harper, J. F. (2005) *Genome Biology* **6,** R77
44. Ubersax, J. A., Woodbury, E. L., Quang, P. N., Paraz, M., Blethrow, J. D., Shah, K., Shokat, K. M., and Morgan, D. O. (2003) *Nature* **425,** 859–864
45. Srinivasan, J., Koszelak, M., Mendelow, M., Kwon, Y. G., and Lawrence, D. S. (1995) *Biochem. J.* **309,** 927–931
46. Rudner, A. D., and Murray, A. W. (2000) *J. Cell Biol.* **149,** 1377–1390
47. Roberts, C. J., Nelson, B., Marton, M. J., Stoughton, R., Meyer, M. R., Bennett, H. A., He, Y. D. D., Dai, H. Y., Walker, W. L., Hughes, T. R., Tyers, M., Boone, C., and Friend, S. H. (2000) *Science* **287,** 873–880
48. Leberer, E., Thomas, D. Y., and Whiteway, M. (1997) *Curr. Opin. Genet. Dev.* **7,** 59–66
49. Krogh, A., Larsson, B., von Heijne, G., Sonnhammer, E. L. (2001) *J. Mol. Biol.* **305,** 567-580.